

---

# 5 Doppler Flow Measurements

As was discussed earlier in [Chapter 2](#), the Doppler effect provides a unique capability for ultrasound to measure blood flow (Evans and McDicken, 2000, Jensen, 1996). Upon insonification by an ultrasound beam, the echoes scattered by blood carry information about the velocity of blood flow. Blood flow measurements are frequently performed in a clinical environment to assess the state of blood vessels and functions of an organ. Ultrasonic Doppler instruments allow a measurement of instantaneous blood flow velocity. Combined with pulse–echo instruments, instantaneous flow rate in a blood vessel as a function of time and cardiac output can be measured noninvasively with ultrasound. At present, very few clinical options are available to do so.

[Figure 5.1](#) shows an ultrasound beam of frequency  $f$  insonifying a blood vessel making an angle of  $\theta$  relative to the velocity,  $v$ . Here it is assumed that blood flows in a vessel with a uniform velocity  $v$ . The returned echoes are Doppler shifted. The Doppler shift frequency,  $f_d$ , is related to the ultrasound frequency,  $f$ , by Equation (2.43):

$$f_d = \frac{2v \cos \theta}{c} f$$

where  $c$  is the sound velocity in blood and may be assumed to be 1540 m/s. The Doppler-shifted frequencies happen to be in the audio range for blood flow velocities in the human body for an ultrasound frequency between 1 and 15 MHz.

Conventionally, two different approaches have been used for ultrasonic Doppler flow measurements: continuous wave (CW) and pulsed wave (PW) Doppler.

## 5.1 NONDIRECTIONAL CW FLOW METERS

A CW system is shown in [Figure 5.2](#). A probe consisting of two piezoelectric elements, one for transmitting the ultrasound signal and one for receiving echoes returned from blood, is excited by an oscillator. The Doppler-shifted echoes are amplified, demodulated, and band-pass filtered to remove the carrier frequency and other spurious signals. Suppose that the ultrasound signal generated by the oscillator is given by  $A \cos(\omega t)$ , where  $A$  denotes signal amplitude and  $\omega$ , the angular frequency,  $= 2\pi f$ . The demodulated signal would be

$$g_d(\omega, \omega_d) = A \cos(\omega t) B \cos[(\omega + \omega_d)t] = \frac{1}{2} AB \{ \cos[(2\omega + \omega_d)t] + \cos(\omega_d t) \}$$

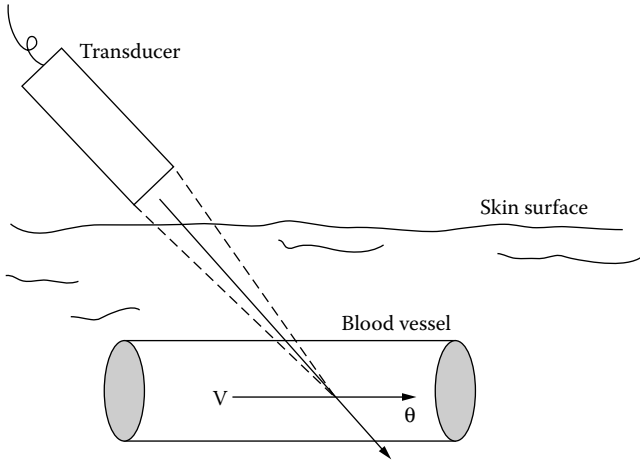


**FIGURE 5.1** An ultrasound beam is incident upon a blood vessel and makes an angle of  $\theta$  relative to the direction of blood flow.

where the echoes are represented by  $B\cos[(\omega + \omega_d)t]$  and  $\omega_d = 2\pi f_d$ . The magnitude of constant  $B$  is determined by the scattering strength of blood.

Much work has been done to better understand the relationship between the Doppler power generated by blood and hematological and hemodynamic factors (Shung et al., 1992; Mo and Cobbold, 1993). Doppler power from blood has been

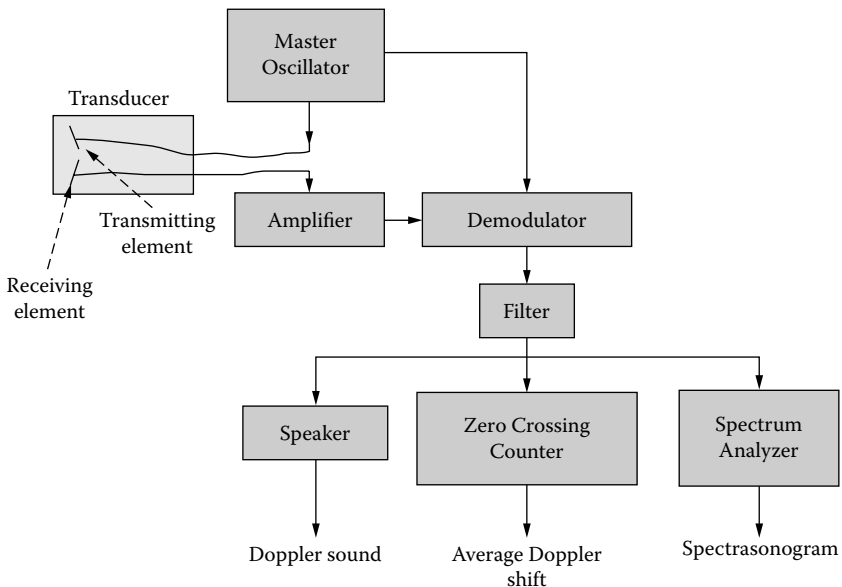


**FIGURE 5.2** Block diagram of a CW Doppler flow meter.

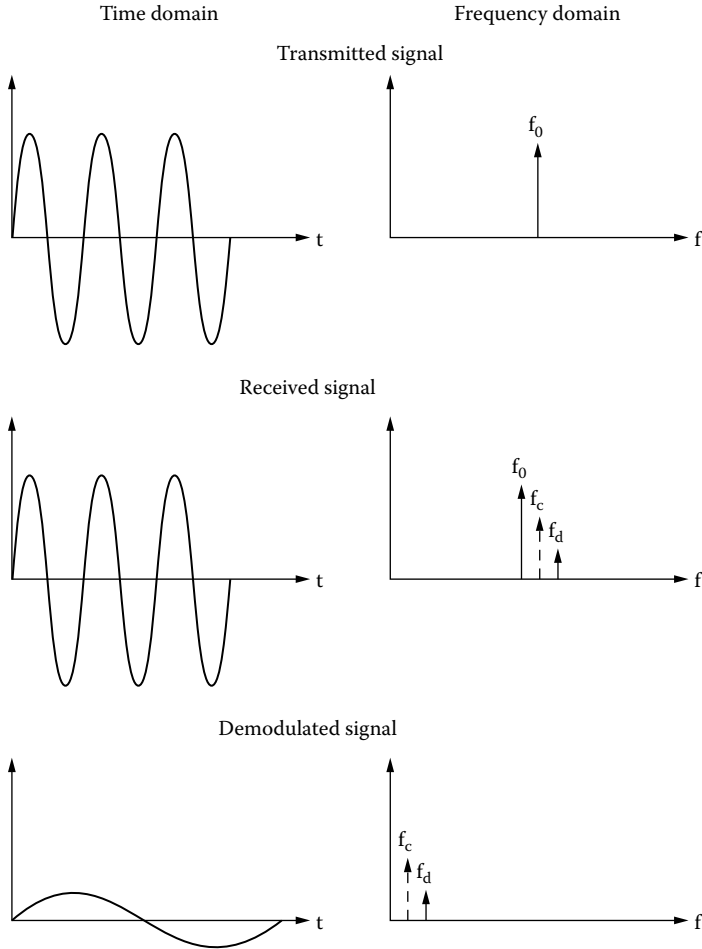


**FIGURE 5.3** Doppler signals in the time and frequency domain showing the effect of demodulation.

found to be related to flow disturbance, hematocrit, and the degree of red blood aggregation; this is in turn affected by the concentration of plasma proteins such as fibrinogen and local shear rate. The output of the demodulator contains the ultrasound carrier frequency and the Doppler shift, as illustrated in Figure 5.3, where the signals in the time and frequency domains are shown on the left and right, respectively. The carrier signal can be readily removed by band-pass filtering by setting the cut-off frequency of the band-pass filter at the high end to be much lower than the carrier frequency.

A problem in ultrasonic Doppler blood flow measurement is that the blood vessels that produce large reflected echoes are slow moving as well. In Doppler terminology, these large, slow-moving echoes are called clutter signals (shown in Figure 5.3 as  $f_c$ ). The cut-off frequency of the band-pass filter at the low end must

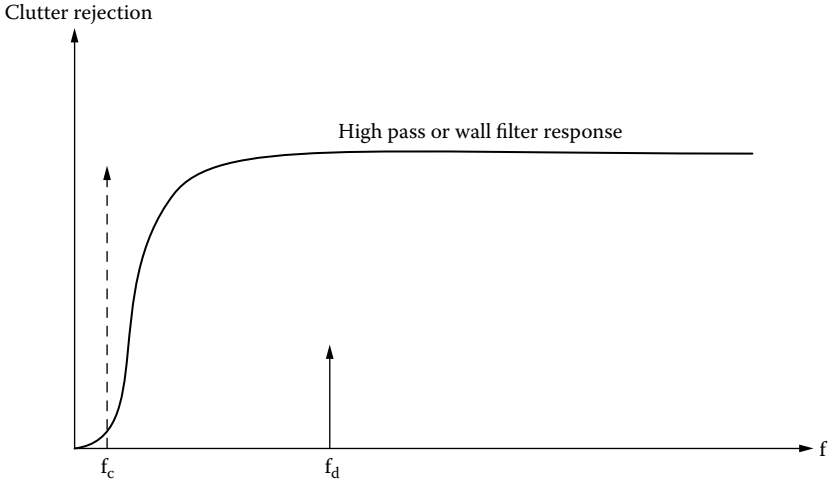


**FIGURE 5.4** Clutter rejection filter or wall filter is used to suppress large echoes produced by slow moving blood vessel walls.

be designed to minimize the interference of these clutter signals. The design of this band-pass filter in the low-frequency region that performs the function of a high-pass (also called clutter rejection) filter has been problematic because the magnitude of clutter signals is several orders higher than those from blood and may mask those from slow moving blood (Figure 5.4). A filter with a very steep slope or a method that carries out some forms of echo cancellation may be used (Jensen, 1996).

The signal after band-pass filtering can be processed in different ways. It may be heard with a speaker because the Doppler shift is in the audible range. Alternatively, a zero-crossing counter can be used to estimate the mean Doppler frequency, or a spectrum analyzer can be used to display the spectrum. The zero-crossing counter estimates the number of zero-crossings of a signal. The number of zero-crossings,  $N$ , and the mean frequency,  $f_m$ , of a signal are given, respectively, by

$$N = 2 \sqrt{\frac{\int_0^{\infty} f^2 P(f) df}{\int_0^{\infty} P(f) df}} \quad (5.1)$$

$$f_m = \frac{\int_0^{\infty} f P(f) df}{\int_0^{\infty} P(f) df} \quad (5.2)$$

where  $P(f)$  is the probability density function at frequency  $f$ . For a pure sinusoidal signal of frequency  $f_m$ ,  $N = 2f_m$ . Complication arises if the signal is not sinusoidal

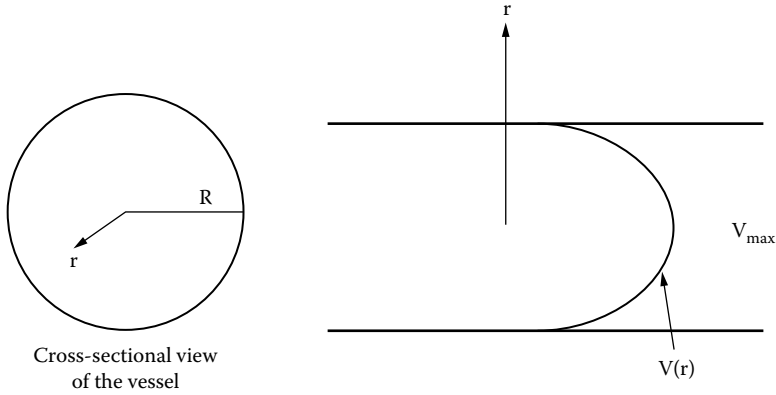


**FIGURE 5.5** Laminar blood flow in an artery has a parabolic flow profile.

as in the case of Doppler flow measurements in which the blood flow is not uniform. For blood flow in a vessel, the velocity is related to radial distance,  $r$ , shown in [Figure 5.5](#), by the following equation (Nichols and O'Rourke, 1990):

$$v(r) = v_{\max} \left[ 1 - \left( \frac{r}{R} \right)^n \right] \tag{5.3}$$

where

- $v_{\max}$  is the peak velocity
- $n$  is an index indicating the nature of flow
- $R$  is the radius of the blood vessel

For parabolic flow,  $n = 2$  and  $N = 1.15 f_{\max}$ , where  $f_{\max}$  is the maximal Doppler frequency.

The spectrum is usually displayed in the format shown in [Figure 5.6](#), in which the vertical axis indicates Doppler frequency or velocity, the horizontal indicates axis time, and the gray scale indicates the intensity of the Doppler signal at that frequency or velocity. At each instant of time, the line displayed represents the Doppler spectrum calculated at that time within a 5- to 10-ms time window. From the Doppler spectrum, the mean frequency or other frequencies (e.g., median frequency) where the Doppler power spectrum is split into two equal halves and mode frequency, where the Doppler power is the highest, can be readily estimated.

Doppler flow meters have been used to assess vascular disorders noninvasively. Flow disturbances near a stenosis cause the Doppler spectrum to broaden because blood flow velocity fluctuates. However, a caveat must be recognized to avoid misdiagnoses: transit time spectral broadening. This is illustrated in [Figure 5.7\(a\)](#) for a single scatterer traversing an ultrasound beam at velocity  $v$ . A finite time is needed for the scatterer to traverse the beam. In the time domain, a finite time duration is

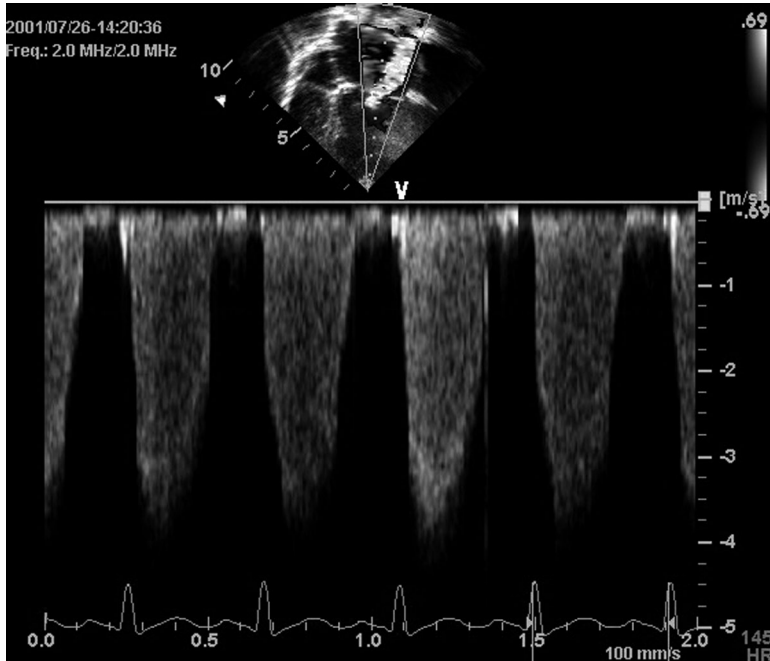


**FIGURE 5.6** Spectrasonogram of CW Doppler signals produced by a mitral valve regurgitation jet. The top image is a B-mode apical four-chamber view of the heart. The dotted line indicates the direction of the Doppler beam. (Courtesy of GE Medical Systems.)

defined by  $\Delta t$  ( $-3$ -dB time duration from peak value) shown in [Figure 5.7\(b\)](#). Translated into the frequency domain, the result is a spectrum with a bandwidth,  $\Delta f$ , purely caused by this transit time effect, instead of a single Doppler spectral line representing velocity  $v$ . This is graphically displayed in [Figure 5.7\(c\)](#).

## 5.2 DIRECTIONAL DOPPLER FLOW METERS

Nondirectional Doppler devices cannot differentiate the direction of blood flow. A few methods have been developed to extract flow direction from the Doppler signal.

### 5.2.1 SINGLE SIDEBAND FILTERING

In [Figure 5.2](#), it is possible to divide the output from the demodulator into two paths. In one path, a high-pass filter is used to filter out signals at frequencies lower than  $f_o$ ; in the other, a low-pass filter is used to filter out signals higher than  $f_o$ , as illustrated in [Figure 5.8](#). In this figure, the portions of the spectrum above and below  $f_o$  are the forward flow and reverse flow Doppler signals, respectively. In this way, the output from one channel contains only forward flow signals and the other contains reverse flow signals. Although this approach is straightforward, the design of the filters can be difficult because the drop-off regions of these filters are very close to  $f_o$ .

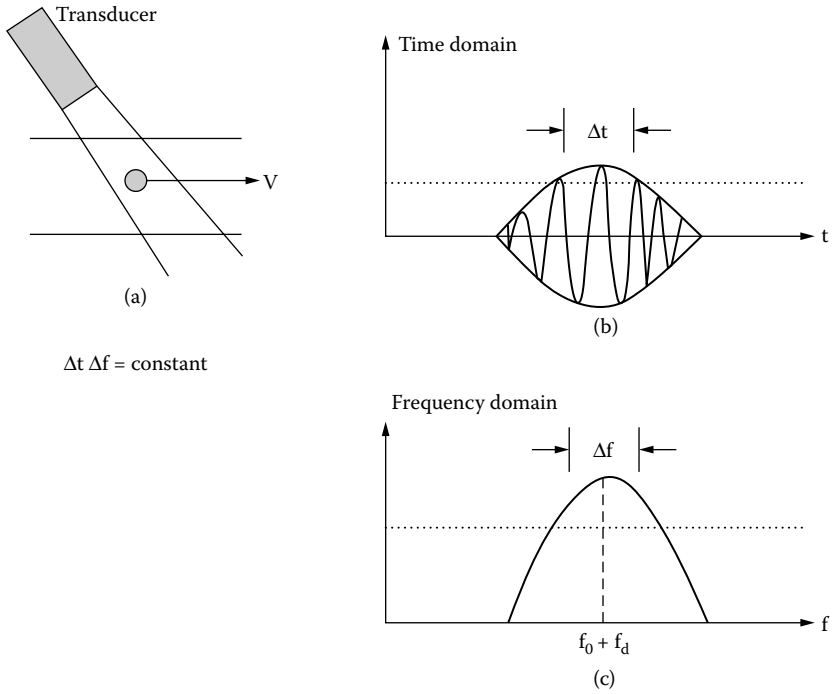


**FIGURE 5.7** Transit time broadening causes an increase in the bandwidth in the frequency domain of the Doppler spectrum.

### 5.2.2 HETERODYNE DEMODULATION

The block diagram of a directional Doppler device that uses heterodyne demodulation is given in Figure 5.9. A heterodyne oscillator generates a sinusoidal signal at a frequency  $f_h$ . The mixer between the oscillator and the heterodyne oscillator

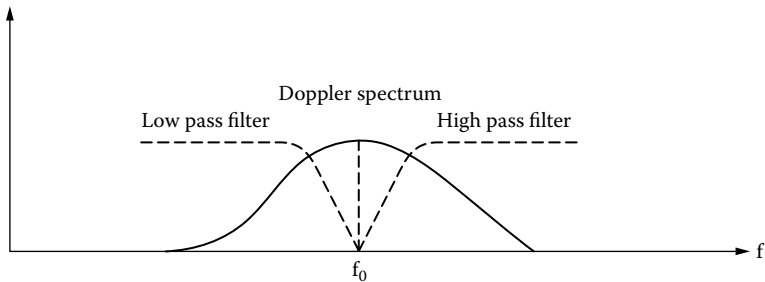


**FIGURE 5.8** Two filters around the carrier frequency can be used to separate forward and reverse flow.

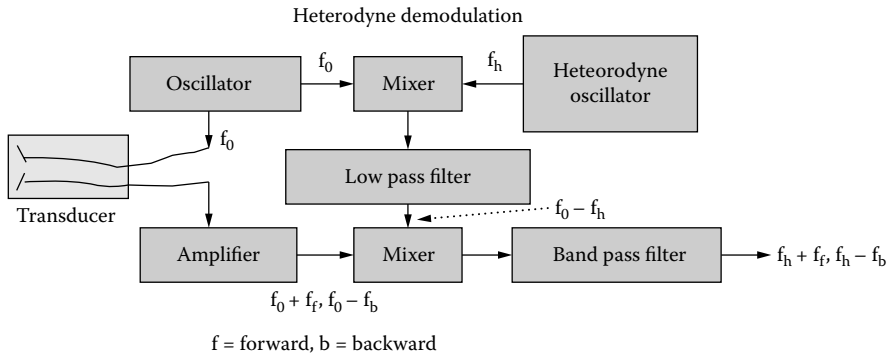


FIGURE 5.9 Block diagram for heterodyne demodulation.

performs a multiplication operation. Its output is given by

$$g_{m1}(\omega_o, \omega_h) = C \cos(\omega_o t) D \cos(\omega_h t) = \frac{1}{2} CD [\cos(\omega_o + \omega_h)t + \cos(\omega_o - \omega_h)t]$$

where  $C$  and  $D$  are the amplitudes of the signals produced by the oscillator and the heterodyne oscillator, respectively.

For the sake of simplicity, assume that  $C = D = 1$  because here only the frequencies are of concern. After low-pass filtering, only the  $\cos(\omega_o - \omega_h)t$  term is left. This signal is then mixed again with the signals detected by the receiving transducer element that contain the Doppler-shifted frequencies in the forward and backward directions,  $f_o - f_b$  and  $f_o + f_f$ . The output of the second mixer is

$$\begin{aligned} g_{m2}(\omega_o, \omega_h, \omega_f, \omega_b) &= \cos(\omega_o - \omega_h)t \cdot [\cos(\omega_o + \omega_f)t + \cos(\omega_o - \omega_b)t] \\ &= \frac{1}{2} [\cos(2\omega_o - \omega_h + \omega_f)t + \cos(2\omega_o - \omega_b - \omega_h)t \\ &\quad + \cos(\omega_h + \omega_f)t + \cos(\omega_h - \omega_b)t] \end{aligned}$$

After low-pass filtering, the signal becomes

$$g_d(\omega_b, \omega_f, \omega_h) = [\cos(\omega_h + \omega_f)t + \cos(\omega_h - \omega_b)t]$$

The effect of heterodyne demodulation in comparison to conventional demodulation in the frequency domain is shown in Figure 5.10.

### 5.2.3 QUADRATURE PHASE DEMODULATION

Figure 5.11 and Figure 5.12 show how quadrature phase demodulation can be used to obtain directional information. Here, it is assumed again that the amplitudes of

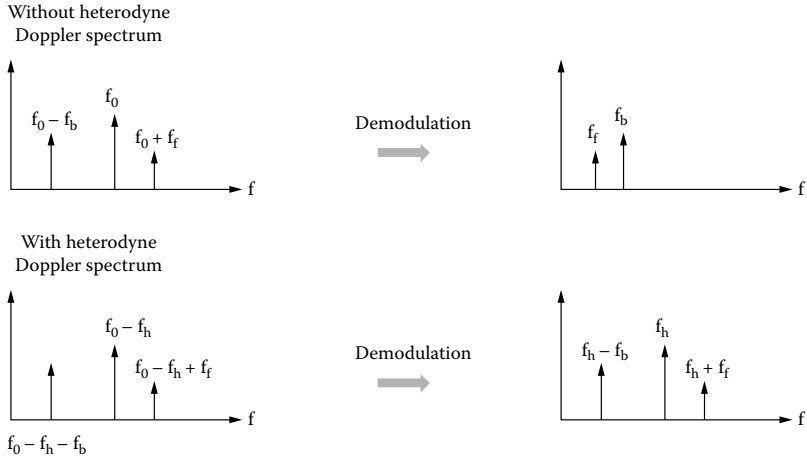


FIGURE 5.10 The effect of heterodyne demodulation in frequency domain.

signals are all equal to 1 to simplify the mathematical operation. The direct channel output is

$$\begin{aligned} & \cos \omega_o t \cdot [\cos(\omega_o + \omega_f)t + \cos(\omega_o - \omega_b)t] \\ &= \frac{1}{2} [\cos(2\omega_o + \omega_f)t + \cos(2\omega_o - \omega_b)t + \cos \omega_f t + \cos \omega_b t] \end{aligned}$$

After low-pass filtering, the signal becomes  $\cos \omega_f t + \cos \omega_b t$ .

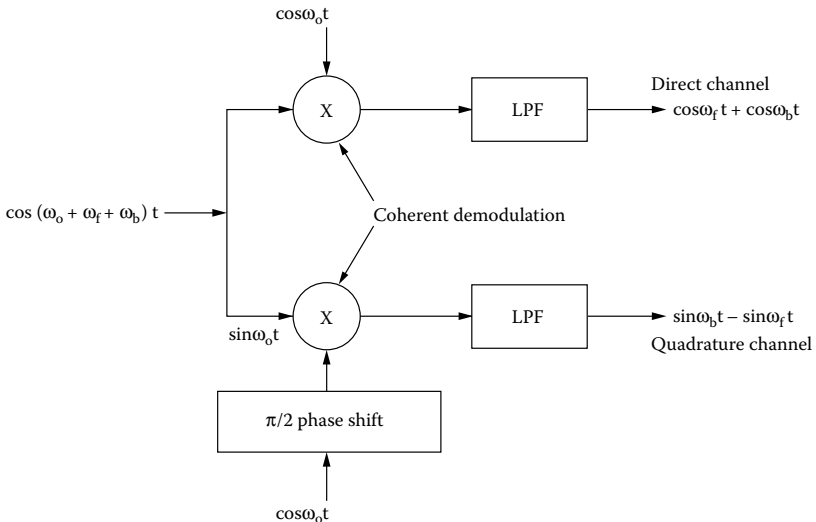
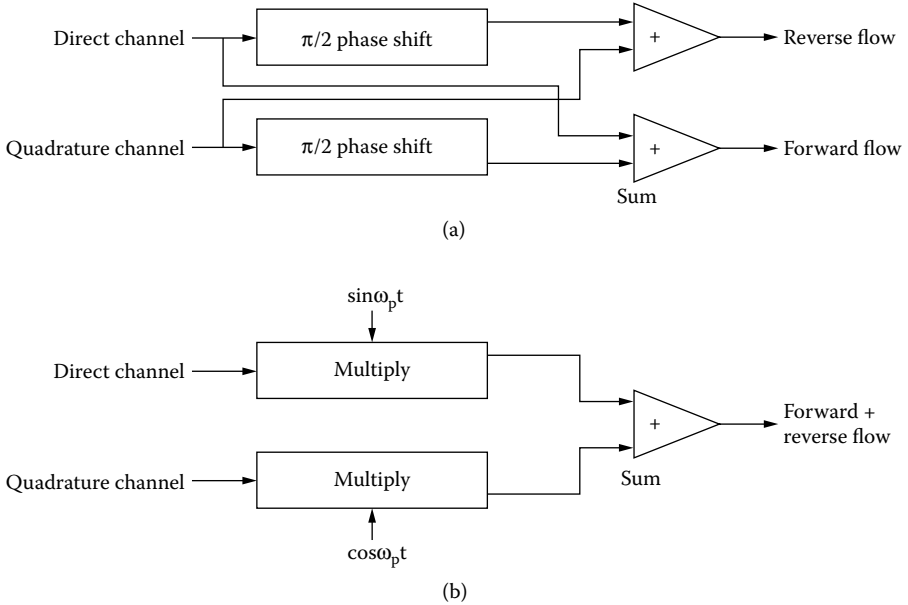


FIGURE 5.11 Quadrature demodulation.



**FIGURE 5.12** Separation of forward and reverse flows can be accomplished in the phase domain (a) and in the frequency domain (b).

The quadrature channel output is

$$\begin{aligned} \cos\left(\omega_o - \frac{\pi}{2}\right)t \cdot [\cos(\omega_o + \omega_f)t + \cos(\omega_o - \omega_b)t] \\ = \sin \omega_o t [\cos(\omega_o + \omega_f)t + \cos(\omega_o - \omega_b)t] \end{aligned}$$

After low-pass filtering, the signal becomes  $-\sin\omega_f t + \sin\omega_b t$ .

To retrieve the directional information from these signals, a phase domain method and a frequency domain method may be used (illustrated in Figure 5.12a and Figure 5.12b, respectively). In the phase domain method, the direct channel output after  $\pi/2$  phase shift is summed with the quadrature channel output to yield the reverse flow signal:

$$D(t) + Q(t + \pi/2) = \cos \omega_f t + \cos \omega_b t - \sin\left(\omega_f t - \frac{\pi}{2}\right) + \sin\left(\omega_b t - \frac{\pi}{2}\right) = 2 \cos \omega_b t$$

The quadrature channel output after  $\pi/2$  phase shift is summed with the direct channel output to yield the forward flow signal,  $2\cos\omega_f t$ .

In the frequency domain method, the direct channel signal is multiplied with a sinusoidal signal,  $\sin\omega_p t$ , and summed up with the quadrature channel signal multiplied by  $\cos\omega_p t$ :

$$D(t) \sin \omega_p t = \sin \omega_p t \cdot [\cos \omega_f t + \cos \omega_b t]$$

$$= \frac{1}{2} [\sin(\omega_p - \omega_f)t + \sin(\omega_p + \omega_f)t + \sin(\omega_p - \omega_b)t + \sin(\omega_p + \omega_b)t]$$

$$Q(t) \cos \omega_p t = \cos \omega_p t \cdot [-\sin \omega_f t + \sin \omega_b t]$$

$$= \frac{1}{2} [\sin(\omega_p - \omega_f)t - \sin(\omega_p + \omega_f)t - \sin(\omega_p - \omega_b)t + \sin(\omega_p + \omega_b)t]$$

Therefore,

$$D(t) \sin \omega_p t + Q(t) \cos \omega_p t = \sin(\omega_p - \omega_f)t + \sin(\omega_p + \omega_b)t$$

### 5.3 PULSED DOPPLER FLOW METERS

A problem with a CW Doppler is its inability to differentiate the origins of the Doppler signals produced within the ultrasound beam. Signals coming from two blood vessels in the same vicinity, e.g., an artery and a vein, may overlap. To alleviate this problem, a pulsed wave Doppler may be used. As illustrated in [Figure 5.13](#), ultrasound bursts of relatively long duration consisting of many cycles

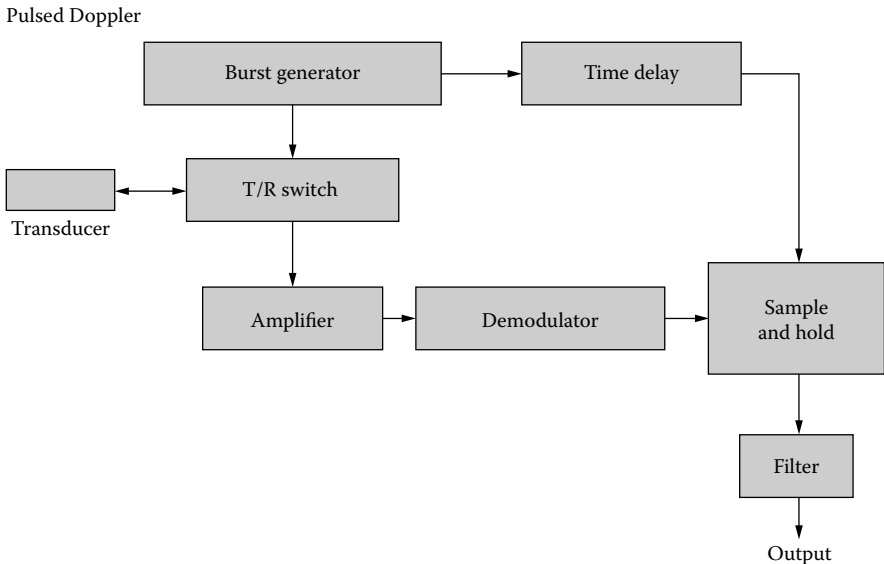
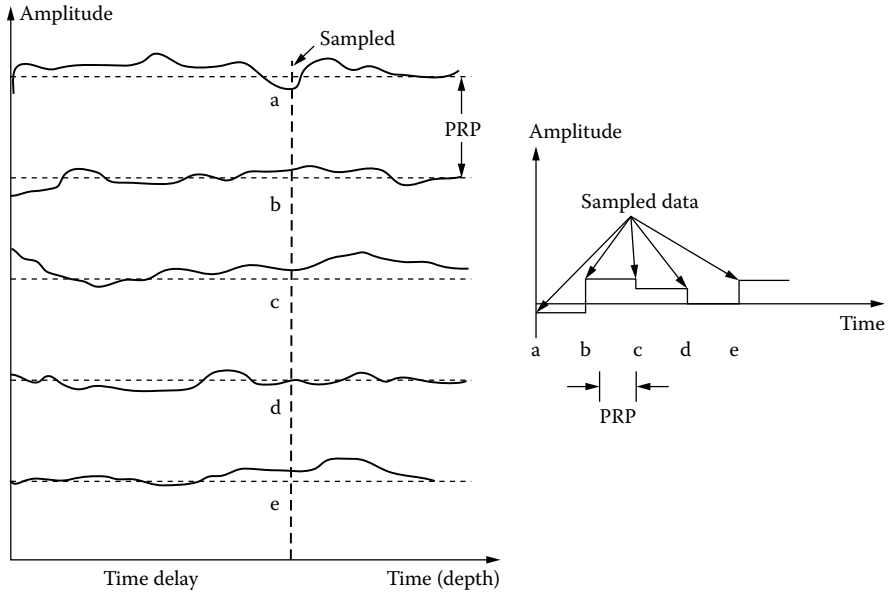


FIGURE 5.13 Block diagram of pulsed Doppler flow meter.



**FIGURE 5.14** Principle used by pulsed Doppler to acquire Doppler signals.

are used to excite the probe. The returned echoes received by the same transducer are amplified and demodulated. The demodulated signal is then sampled and held by a sample-and-hold circuit, which is triggered by the delayed pulses. The time-delayed pulses allow the selection of the location where the Doppler shift frequency is monitored.

Figure 5.14 illustrates the principle behind pulsed Doppler flow meters. Each waveform in the left panel represents the echo waveform received by the transducer after a burst is transmitted. The waveforms are separated by the pulse repetition period (PRP). The time delay is set to allow the sampling of the waveform at points a, b, c, d, and e. The sample-and-hold circuit samples the waveforms at these points and holds the voltage at the sampled level until the next sampling time, as illustrated in the right-hand panel. Following band-pass filtering, the Doppler signal can be displayed or heard as the CW Doppler.

A drawback of the pulsed Doppler is the limit of the highest Doppler frequency or maximal velocity that it can measure. This is determined by the pulse repetition frequency (PRF) of the device, which must be at least twice as large as the maximal Doppler frequency. This may pose a problem when measuring high velocities in the body, e.g., outflow tracts of cardiac valves and stenosis in a blood vessel. To avoid aliasing, the PRF of the pulsed Doppler device must be

$$PRF > 2f_{\max}$$

$$\therefore PRF > (4v_{\max}f)/c \quad (5.4)$$

where  $f_{\max}$  and  $v_{\max}$  are the maximal Doppler shift frequency and maximal velocity, respectively. To avoid range ambiguity, all echoes must be received before the next burst is transmitted, i.e.,

$$PRP = \frac{1}{PRF} > \frac{2z_{\max}}{c} \quad (5.5)$$

where  $z_{\max}$  is the maximal depth of penetration. Combining Equation (5.4) and Equation (5.5),

$$v_{\max} \cdot z_{\max} \leq \frac{c^2}{8f} \quad (5.6)$$

The term on the right side of the equation is a constant. This means that the performance of the pulsed Doppler device is limited by the maximal velocity that it can detect or the maximal depth of penetration. To enhance one, the performance of the other must be compromised. Modern high-end ultrasonic imaging machines are equipped with CW and PW capabilities.

## 5.4 CLINICAL APPLICATIONS AND DOPPLER INDICES

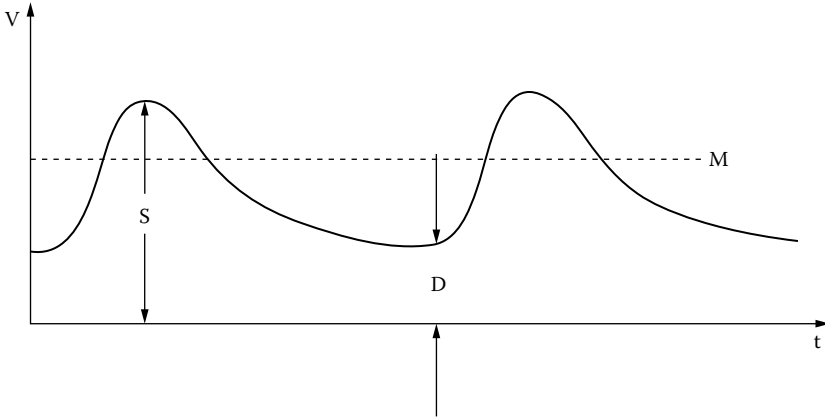
Ultrasonic Doppler devices are inexpensive and are capable of yielding clinically useful information noninvasively. Their primary applications have been in assessing cardiovascular systems, e.g., diagnosing stenosis in blood vessels and cardiac valvular diseases. They have also been used to estimate cardiac valvular stenosis (Feigenbaum, 1986). The velocity measured by the Doppler devices depends upon the Doppler angle, which is difficult to estimate; therefore, a few indices that are not angle dependent have been used frequently in a clinical setting to derive useful diagnostic data.

Figure 5.15 shows the mean velocity waveform from a peripheral artery obtained with a CW Doppler flow meter. The pulsatility index is defined as the ratio of  $(S - D)/M$ , where  $S$ ,  $D$ , and  $M$  are the peak, minimal, and mean velocities, respectively. In this expression, the angle dependence is eliminated. The pulsatility index has been found to be related to the resistance of the vessel downstream from the measurement site. Another useful index is the Purcelot resistance index for the carotid artery, which is defined as  $(S - D)/S$ .

## 5.5 POTENTIAL PROBLEMS IN DOPPLER MEASUREMENTS

In Doppler flow measurements, preventive measures must be taken to avoid errors that may result from the following problems:

- Erroneous Doppler angle estimation
- Nonuniform insonification of vessel by the ultrasound beam



**FIGURE 5.15** Mean velocity waveform acquired with a CW flow meter from a peripheral blood vessel can be used to derive indices useful for diagnosing vascular diseases.

- Aliasing of Doppler frequency estimation
- Intrinsic spectral broadening
- Attenuation of intervening tissues between the probe and the region of interest
- Clutter signals generated by slow moving large anatomical structures

The Doppler angle can be better estimated with the aid of B-mode imaging, although it is still not ideal because of the tortuosity of blood vessels. If the sensitive volume of the ultrasound beam or beams is smaller than the vessel, portions of the blood will not be included in the measurement, resulting in estimated velocity values that may deviate from the true values. Because the attenuation of tissues is linearly proportional to frequency, the Doppler spectrum may be affected if deeper tissues are interrogated. Other problems have been addressed in preceding sections.

## 5.6 TISSUE DOPPLER AND MULTIGATE DOPPLER

In the Doppler signal processing chain shown in [Figure 5.2](#) and [Figure 5.13](#), if only large amplitude echoes of lower Doppler frequencies from tissues such as myocardium or heart muscle are retained and low amplitude echoes of higher Doppler frequencies are suppressed, the motion of the tissues can be monitored. This will be touched upon again in the next chapter. An amplitude threshold can be set to allow only the larger echoes to pass through. Tissue Doppler has been proven a clinically useful tool for assessing the state of myocardium.

In conventional pulsed Doppler, only one gate is used to measure blood flow within the sampled window or sampling volume confined by the beam width and the gate duration. If blood flow velocities at multiple points along the ultrasound beam need

to be measured, pulsed Doppler flow meters with multiple gates (e.g., 8 or 16 gates) have been developed. These devices allow the measurement of velocities in real time across the lumen and thus have been used frequently to determine the blood flow velocity profile in arteries.

## REFERENCES

- Evans, D.H. and McDicken, W.N. *Doppler Ultrasound: Physics, Instrumentation and Signal Processing*. Wiley: New York, 2000.
- Feigenbaum, H. *Echocardiography*, 4th ed. Philadelphia: Lea and Febiger, 1986.
- Jensen, J.A. *Estimation of Blood Velocities Using Ultrasound*. Cambridge: Cambridge University Press, 1996.
- Mo, L.Y.L. and Cobbold, R.S.C. Theoretical models of ultrasonic scattering in blood. In Shung, K.K. and Thieme, G.A., Eds. *Ultrasonic Scattering in Biological Tissues*, Boca Raton, FL: CRC Press, 1993, 125–170.
- Nichols, W.W. and O'Rourke, M.F. *McDonald's Blood Flow in Arteries*. Philadelphia: Lea and Febiger, 1990.
- Shung, K.K., Cloutier, G., and Lim, C.C. The effects of hematocrit, shear rate, and turbulence on ultrasonic Doppler spectrum from blood. *IEEE Trans. Biomed. Eng.* 1992, 39:462–469.